



Biochem. J. (2013) 453, 357-370 (Printed in Great Britain) doi:10.1042/BJ20130529





The polyserine domain of the lysyl-5 hydroxylase Jmid6 mediates subnuclear localization

Alexander WOLF*1, Monica MANTRI†1, Astrid HEIM‡, Udo MÜLLER‡, Erika FICHTER‡, Mukram M. MACKEEN†2, Lothar SCHERMELLEH‡§, Gregory DADIE||, Heinrich LEONHARDT‡, Catherine VÉNIEN-BRYAN||, Benedikt M. KESSLER¶. Christopher J. SCHOFIELD^{†1,3} and Angelika BÖTTGER^{‡1,3}

*Institute of Molecular Toxicology and Pharmacology, Helmholtz Zentrum München-German Research Center for Environmental Health, Ingolstädter Landstrasse 1, 85764 Neuherberg, Germany, †Chemistry Research Laboratory and Oxford Centre for Integrative Systems Biology, University of Oxford, 12 Mansfield Road, Oxford OX1 3TA, U.K., ‡Department of Biology II, Ludwig Maximilians University, Munich, Grosshaderner Strasse 2, 82152 Planegg-Martinsried, Germany, §Department of Biochemistry, University of Oxford, South Parks Road, Oxford OX1 3QU, U.K., ||IMPMC, UMR7590, CNRS, Université Pierre et Marie Curie, Case 115, 4 place Jussieu, 75252 Paris Cedex 05, France, and ¶Henry Wellcome Building for Molecular Physiology, Nuffield Department of Medicine, University of Oxford, Oxford OX3 7BN, U.K.

Jmjd6 (jumonji-domain-containing protein 6) is an Fe(II)and 2OG (2-oxoglutarate)-dependent oxygenase that catalyses hydroxylation of lysine residues in proteins involved in premRNA splicing. Jmjd6 plays an essential role in vertebrate embryonic development and has been shown to modulate alternative splicing in response to hypoxic stress. In the present study we show that an alternatively spliced version of Jmjd6 lacking the polyS (polyserine) domain localizes to the nucleolus, predominantly in the fibrillar centre. Jmjd6 with the polyS domain deleted also interacts with nucleolar proteins. Furthermore, coimmunoprecipitation experiments and F2H (fluorescent 2-hybrid)

assays demonstrate that Jmjd6 homo-oligomerization occurs in cells. In correlation with the observed variations in the subnuclear distribution of Jmjd6, the structure of Jmjd6 oligomers in vitro changes in the absence of the polyS domain, possibly reflecting the role of the polyS domain in nuclear/nucleolar shuttling of Jmid6.

Key words: Fe(II)- and 2-oxoglutarate-dependent oxygenase, JmjC, lysine hydroxylation, nucleolus, polyserine domain, pre-mRNA splicing.

INTRODUCTION

Jmjd6 (jumonji-domain-containing protein 6) is highly conserved throughout animal evolution and plays an important role in embryonic development. Various Jmjd6 loss-of-function experiments in vertebrates displayed severe developmental defects and embryonic lethality (reviewed in [1]). Jmjd6 is an Fe(II)- and 2OG (2-oxoglutarate)-dependent oxygenase that catalyses hydroxylation of lysine residues in splicing-associated proteins and modulates alternative splicing [2-4]. One established target of Jmjd6 is splicing factor U2AF65 (U2 small nuclear ribonucleoprotein auxiliary factor 65-kDa subunit) [4]. Recently Jmjd6 has been suggested to be also involved in epigenetic regulation via hydroxylation of lysine residues in histones [5].

In addition to the 'catalytic' JmjC domain of Jmjd6, conserved sequence motifs are present; these include NLSs (nuclear localization sequences), an AT-hook motif (residues Lys300-Ser³⁰⁹) and a SUMOylation site (Leu³¹⁶–Glu³¹⁹) [6,7]. Jmjd6 also contains a polyS (polyserine) region comprising 16 serine residues interrupted by four aspartate residues (Ser³⁴⁰–Ser³⁵⁹). Jmjd6 splice variants have been reported which lack this polyS region [7]. The Jmjd6 polyS region is highly conserved [8] and expected to be largely unstructured [9,10].

In some bacterial extracellular modular carbohydratedegrading enzymes, polyS regions have been predicted to act as flexible linkers, which connect substrate binding and enzymatic domains [11]. Similar to Jmjd6, some of the eukaryotic serinecontaining proteins are linked to pre-mRNA splicing, e.g. SRrp37 and RNPS1 [12,13]. However, the function of the polyS domains is unknown in these proteins.

Many 2OG oxygenases form dimers, for instance, homodimerization of FIH [factor inhibiting HIF (hypoxia-inducible factor)] [14], the catalytic domain of which is related to that of Jmjd6, is mediated by two C-terminal α -helices [15] and is required for substrate binding [16]. 2OG oxygenases and related enzymes can also exist in oligomeric forms, including tetramers [17] and hexamers [18]. A crystal structure of a C-terminally truncated form of human Jmjd6, lacking residues 344-403, showed homodimerization via the N-terminal helix 4 (residues Glu⁶¹-Lys⁶⁸) and the C-terminal helix 13 (Glu³²²-Gln³³⁴) of each subunit, which form a 'pseudo-4-helix bundle' [19]. A second crystal structure of full-length Jmjd6 revealed a monomeric form [10]; however, this structure was in complex with a Fab fragment, which may have hindered dimerization. Evidence for higher order oligomers of Jmjd6 has also been described in solution studies [20-22].

Abbreviations used: BHK, baby hamster kidney; BIFC, bimolecular fluorescence complementation; co-IP, co-immunoprecipitation; 3D-SIM, 3D structured illumination microscopy; DFC, dense fibrillar centre; F2H, fluorescent 2-hybrid; FC, fibrillar centre; FLIP, fluorescence loss in photobleaching; fps, frames/s; GC, granular centre; HA, haemagglutinin; HEK, human embryonic kidney; Jmjd6, jumonji-domain-containing protein 6; LSM, SM-like; MIG, mitotic interchromatin granule; MS/MS, tandem MS; NLS, nuclear localization sequence; 2OG, 2-oxoglutarate; polyS, polyserine; SEC, size-exclusion chromatography; snRNA, small nuclear RNA; TEM, transmission electron microscopy; UBF, upstream binding factor; UPLC, ultra performance liquid chromatography.

¹ These authors contributed equally to this work.

² Present address: School of Chemical Science, Faculty of Science and Technology, Universiti Kebangsaan Malaysia, 43600 Bangi, Selangor Darul

Correspondence may be addressed to either of these authors (email christopher.schofield@chem.ox.ac.uk or boettger@zi.biologie.uni-muenchen.de).

In the present paper we report cell-based studies demonstrating that the Jmjd6 polyS domain is involved in bidirectional nucleoplasmic–nucleolar shuttling of Jmjd6 and that its presence/absence regulates subnuclear localization of Jmjd6. TEM (transmission electron microscopy) studies show that the overall oligomeric structure of Jmjd6 changes from rings to fibrils when the polyS domain is deleted. We propose that the effects of the polyS domain on Jmjd6 structure are linked to its role in regulating localization.

EXPERIMENTAL

Cell culture, transfection and immunostaining

HeLa cells and HEK (human embryonic kidney)-293T cells were cultured in DMEM (Dulbecco's modified Eagle's medium) supplemented with 10% FBS, penicillin (100 units/ml) and streptomycin (100 μ g/ml) at 37 °C with 5 % CO₂. For microscopy, HeLa cells were grown to 50-70 % confluence on $18 \text{ mm} \times 18 \text{ mm}$ glass coverslips and transfected with expression constructs using LipofectamineTM 2000 (Invitrogen) according to the manufacturer's instructions. At 24 h post-transfection, cells were fixed with 4% paraformaldehyde (15 min at room temperature) and permeabilized with 1% Triton X-100 in PBS. Mouse anti-UBF (upstream binding factor) (SC-13125, Santa Cruz Biotechnology), mouse anti-SC35 (ab11826, Abcam), rabbit anti-UBTF (HPA006385, Sigma) and mouse anti-Jmjd6 (mAB328) [20] were used as primary antibodies, Cy3 (indocarbocyanine)coupled anti-mouse (Jackson Immuno Research), Alexa Fluor® 647-coupled anti-mouse (Invitrogen) and Alexa Fluor® 488coupled anti-rabbit (Invitrogen) were used as secondary antibodies.

TEM

Jmjd6 constructs were cloned into the pET28b(+) vector and then expressed with an N-terminal His tag in Escherichia coli, with purification using a nickel affinity column as described previously [4]. In order to avoid aggregation of protein over the time and by repeated freeze-thaw cycles, once purified, the protein was concentrated and then buffer exchanged with a low glycerol concentration buffer (50 mM Tris/HCl, 300 mM NaCl and 5% glycerol, pH 7.5) using Micro BioSpin columns (Bio-Rad Laboratories). Sample grids for TEM analysis were prepared immediately after protein preparation. Jmjd6 (wild-type or truncated constructs) was applied at 0.03 mg/ml to TEM grids and stained with 2% uranyl acetate. Electron micrographs were recorded (×45000) using a FEI-Phillips CM120 EM. Images were digitized on a Nikon Super Coolscan 9000 [step size of 12.5 μ m with a pixel size of 2.78 Å (1 Å = 0.1 nm)]. WEB and SPIDER software [23] were used for image processing. A total of 4736 particles were windowed, subjected to reference-free alignment, and sorted into classes using the K-means clustering [24].

SEC (size-exclusion chromatography)

Gel-filtration chromatography was performed at 4°C using a 30 ml Superdex 200 column and an ÄKTA purifier FPLC (GE Healthcare) using 20 mM Hepes, pH 7.5, as elution buffer at a flow rate of 0.8 ml/min. The gel-filtration column was calibrated using 20 mM Hepes, pH 7.5, with molecular mass markers (blue dextran, 2000 kDa; bovine thyroglobulin, 669 kDa; equine apoferritin, 443 kDa; *Streptomyces cattleya* ThnG, 291 kDa;

and cytochrome c, 12.3 kDa). Protein elution was monitored at 280 nm and results were analysed using Unicorn software (version 5.10).

Co-IP (co-immunoprecipitation) experiments

HeLa cells were transiently transfected with HA (haemagg-lutinin)-tagged full-length Jmjd6 and either GFP or a GFP-tagged Jmjd6 variant. The GFP-nanotrap (ChromoTek) has been used for immunoprecipitation as described previously [4]. Primary antibodies for Western blotting were mouse anti-GFP antibody (11814460001, Roche) and rabbit anti-HA antibody (H6908, Sigma).

F2H (fluorescent 2-hybrid) assay

Transgenic BHK (baby hamster kidney) cells (clone 2) containing lac-operator repeats [25] were transiently transfected with Jmjd6-pF2H-bait (triple fusion protein of Jmjd6, RFP and lac repressor) [26] and co-transfected with either NLS-GFP, Histone 2B-GFP, Jmjd6-GFP or an inactive Jmjd6 variant (H187A/D189A)-GFP. Formaldehyde-fixed (3.7 % in PBS) cells were analysed 24 h post-transfection by using a Leica TCS SP5 II.

2D gel analysis

HEK-293T cells expressing HA-tagged Jmjd6 were lysed with lysis buffer (20 mM Tris/HCl, pH 8.0, 150 mM NaCl and 0.5 % Nonidet P40 supplemented with protease [Pefabloc® (Boehringer), $10~\mu g/ml$ pepstatin A, $10~\mu g/ml$ aprotinin and $10~\mu g/ml$ leupeptin] and phosphatase inhibitors [100 nM okadaic acid and phosphatase inhibitor cocktails 1 and 2 (Sigma)]. Lysate was loaded on to a non-denaturing native gel [7 % acrylamide/bisacrylamide (29:1) and 80 mM Tris/HCl, pH 7.3]. The entire native gel lane was excised and either boiled (95 °C, 5 min in SDS loading buffer) or not, then analysed by SDS/PAGE (10 % gel). Proteins were immunoblotted and detected by an anti-Jmjd6 antibody (ab10526, Abcam).

3D-structured illumination microscopy

HeLa cells were fixed for 10 min with 2% formaldehyde and washed with PBST (0.02% Tween 20 in PBS). Cells were quenched in saturated glycine solution and permeabilized for 10 min with 0.5% Triton X-100 in PBS. Blocking was performed in 2% BSA and 0.5% fish skin gelatin. Primary antibodies used for immunostaining were: rabbit anti-Jmjd6 (ab10526, Abcam) and mouse anti-SC35 (ab11826, Abcam). Secondary antibodies (Invitrogen) were coupled to Alexa Fluor® 488 and Alexa Fluor® 594. To enhance GFP signals, the GFP-Booster_Atto488 (ChromoTek) was used. Cells were post-fixed with 4% formaldehyde in PBS and counterstained with 200 ng/ml DAPI in PBST for 10 min. Cells were mounted on to microscopy slides with Vectashield mounting medium (Vector Laboratories) and imaged using the DeltaVision OMX microscope (Applied Precision).

In-gel trypsin digestion

Trypsin digestion of samples run on 4–12% NuPage gels (Invitrogen) were prepared for MS analysis as described previously [27]. In brief, gel bands stained with Coomassie Blue (ImperialTM Protein Stain, Thermo/Pierce) were cut into

small pieces (approximately 1 mm³). Destaining solution (50 % methanol and 5 % acetic acid) was added, and the solution was shaken (~ 350 rev./min) for 2–3 h, the destaining solution was then removed, 200 μ l of the same solution was added and left overnight under the same conditions. The destaining solution was then removed, 200 μ l of acetonitrile was added and the solution was left for 5–15 min (until the gel pieces had shrunk and whitened). The acetonitrile was then pipetted off and the gel pieces were dried by centrifugation in vacuo (Heto/Eppendorf vacumn concentrator) for 5 min. Subsequently, reduction was carried out with DTT (10 mM), followed by alkylation with iodoacetamide (100 mM). Trypsin digestion for MS analysis was then carried out whereby the excised gel pieces, which were subjected twice to hydration and dehydration using destaining solution and acetonitrile respectively, followed by overnight incubation at 37 °C with trypsin (20 ng/ μ l) in 100 mM ammonium bicarbonate (pH 7.8) digestion buffer. The final samples were redissolved in 0.1 % formic acid and 2 % acetonitrile and stored at -20 °C until analysis.

Protein analysis by MS

The digested material was subjected to nano-UPLC (ultra performance liquid chromatography)-MS/MS (tandem MS) analysis using a 75 μ m-inner diameter×25 cm C₁₈ nanoAcquityTM UPLCTM column (1.7- μ m particle size; Waters) and a 90 min gradient of 2-45% solvent B (solvent A, 99.9% H₂O and 0.1% formic acid; solvent B, 99.9% acetonitrile and 0.1% formic acid) on a Waters nanoAcquity UPLC system [final flow rate, 250 nl/min; 7000 psi (1 psi = 6.9 kPa)] coupled to a Q-TOF Premier tandem mass spectrometer (Waters) run in positive ion mode. MS analysis was performed in DDA (datadirected analysis) mode (MS to MS/MS switching at precursor ion counts greater than 1 and MS/MS collision energy dependent on precursor ion mass and charge state). All raw MS data were processed using the PLGS software (version 2.3), including deisotoping and deconvolution (converting masses with multiple charge states to m/z = 1). The mass accuracy of the raw data was corrected using Glu-fibrinopeptide (200 fmol/\mu1; 700 nl/min flow rate; 785.8426 Da $[M + 2H]^{2+}$) that was infused into the mass spectrometer as a lock mass during analysis. MS and MS/MS data were calibrated at intervals of 30 s. MS/MS spectra (peak lists) were searched against the UniProtKB/Swiss-Prot human database using Mascot version 2.3.01 (Matrix Science) and the following parameters: peptide tolerance, 0.2 Da; ${}^{13}C = 1$; fragment tolerance, 0.1 Da; missed cleavages, 2; instrument type, ESI-Q-TOF; fixed modification, carbamidomethylation (C); and variable modifications, deamidation (N, Q) and oxidation (M, K). The interpretation and presentation of MS/MS data were performed according to published guidelines [28].

FRAP and FLIP (fluorescence loss in photobleaching)

FRAP and FLIP experiments were performed on an UltraView VoX spinning disk microscope system (PerkinElmer) using a $63\times/1.4$ numerical aperture Plan Apochromat oil-immersion objective. The system was equipped with a heated environmental chamber set to 37 °C and CO₂ perfusion set to 5 %. For FRAP experiments, time series were recorded with the 488 nm laser attenuated to 20 % transmission and exposure times of 147 ms. For each FRAP experiment, 20 prebleach timepoints were recorded before bleaching a nucleolar spot of 3 μ m diameter for 0.67 s with the 488 nm laser set to 100 % transmission. Fluorescence recovery was then followed for 200 timepoints

at a rate of 6.6 fps (frames/s) and 180 timepoints at a rate of 1.9 fps. FRAP experiments were quantitatively analysed using ImageJ (NIH) as described previously [29]. Series were converted into 8-bit and Gauss-filtered (2 px radius). The mean fluorescence intensity of the bleached and unbleached regions were background subtracted and normalized. The results of at least 16 measurements were averaged for each construct. For each time series the half-time of recovery was determined and the mean \pm S.E.M. was calculated. For FLIP analyses a defined nucleoplasmic spot of 3 μ m diameter was constantly bleached every 0.4 s. Fluorescence intensity in a nucleolar region was analysed over 45 s.

BIFC (bimolecular fluorescence complementation) assay

The full-length human Jmjd6 sequence was cloned into YN and YC plasmids respectively, as described previously [30]. YC-Fos and YN-Jun were used as control plasmids, as they have been shown to interact previously [30]. BIFC analyses were performed in HeLa cells.

Reverse transcription–PCR for amplification of alternatively spliced *JMJD6* mRNA

Total RNA was isolated from HeLa cells, reverse transcribed and amplified with primers hybridizing in exon 3 (5') and 5 or 6 (3') respectively. The PCR products were sequenced and revealed the presence of a Jmjd6 splice variant, including alternative exon 5. In order to obtain the complete 3'-sequence of this splice variant, PCR was carried out with exon 3 and oligo(dT) primers. After sequencing, the presence of cDNA encoding the Jmjd6 splice variant Hs3 [7] was confirmed.

RESULTS

Jmjd6 is localized in the nucleoplasm and to a lesser extent in the nucleolus

High-resolution microscopy and 3D-SIM (3D structured illumination microscopy) reconstruction [31] of HeLa cell nuclei stained with an anti-Jmjd6 antibody revealed the exclusively nuclear distribution of the Jmjd6 protein. Co-staining with an antibody against SC35, a general marker for interchromatin granule clusters, demonstrates that the majority of Jmjd6 is not associated with nuclear speckles (Figure 1A). Moreover, the images indicate the presence of some endogenous Jmjd6 in the nucleoli. Nucleolar Jmjd6 localization is more apparent in cells overexpressing GFP-tagged Jmjd6, which was found inside the nucleoli in well-defined dots (Figure 2A).

We also observed that the relative amount of nucleolar Jmjd6 varies in different cell lines, being slightly stronger in mouse C2C12 cells than in HeLa cells. Moreover, the nucleolar signal was dependent on the anti-Jmjd6 antibodies we used. A strong Jmjd6 signal in nucleoli was detected with antibodies raised against epitopes within the first 300 amino acids of the wild-type Jmjd6 sequence, for instance, anti-Jmjd6 antibody sc-28348 (Santa Cruz Biotechnology) or mAB328 [20]. In contrast, the anti-Jmjd6 antibody ab10526 (Abcam), which recognizes an epitope in the C-terminal part of Jmjd6 (amino acids 364–372) [20], led to the observation of very little nucleolar anti-Jmjd6 staining (Figures 1B–1F). These observations motivated us to investigate the role of the different Jmjd6 domains in determining subnuclear localization.

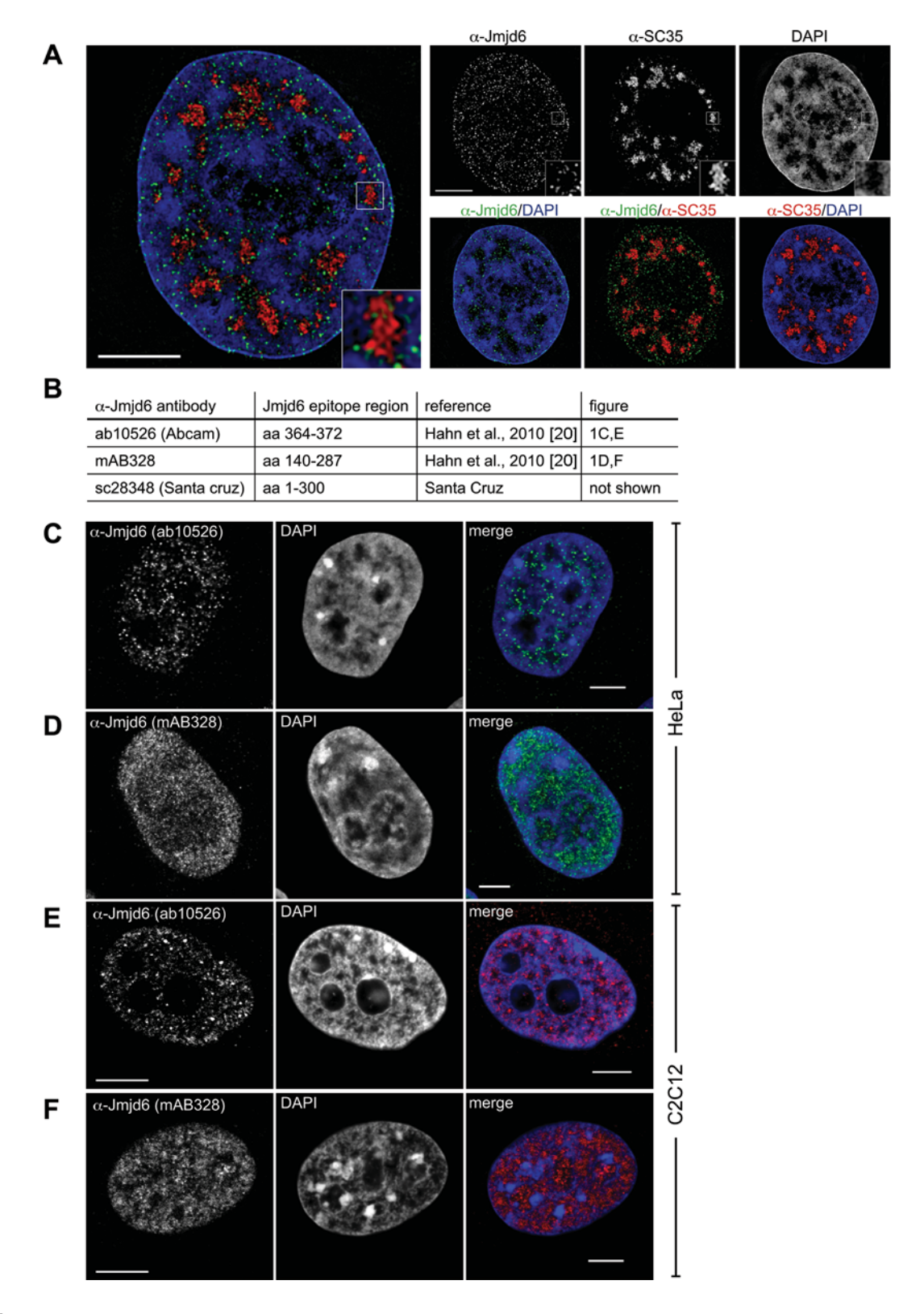


Figure 1 Subnuclear localization of endogenous Jmjd6

(A) Localization of endogenous Jmjd6 in the nucleus of HeLa cells using super-resolution 3D-SIM imaging. SC35 adopts a speckled distribution in the interchromatin space, whereas endogenous Jmjd6 is homogenously distributed throughout the nucleoplasm. Cells are immunostained with antibodies against Jmjd6 (green) and SC35 (red). DNA is counterstained with DAPI (blue). The central mid-section of a HeLa cell nucleus is shown (scale bar, 5 μ m). (B) Table of anti-Jmjd6 antibodies targeting different epitope regions in Jmjd6. (C and E) Staining of either HeLa (C) or C2C12 cells (E) with the ab10526 anti-Jmjd6 antibody gives a very weak nucleolar signal. (D and F) In contrast, the mAB328 staining reveals a strong anti-Jmjd6 pattern in the nucleoli of both cell types. (C-F) Central mid-sections of HeLa or C2C12 cell nuclei (scale bars, 5 μ m). DNA is counterstained with DAPI.

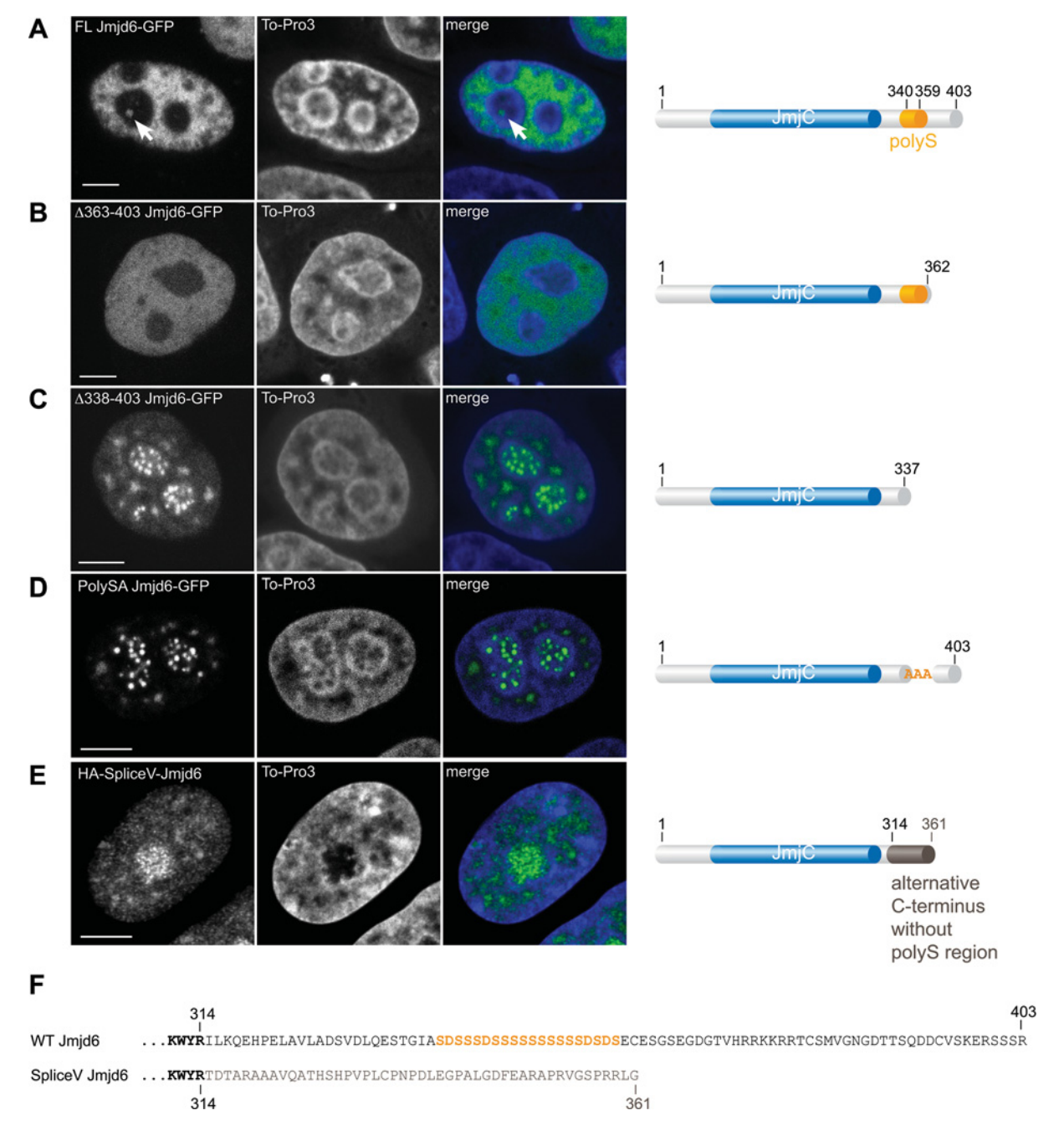


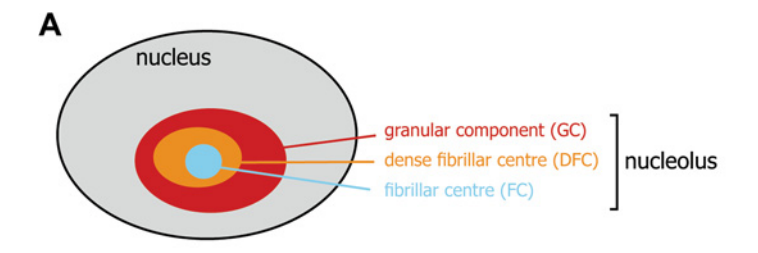
Figure 2 Intracellular distribution of Jmjd6 depends on its polyS region

 $(\mathbf{A}-\mathbf{E})$ Confocal sections of HeLa cells expressing GFP-tagged Jmjd6 variants. DNA is counterstained with T0-PR03 (Scale bars, $5~\mu$ m). (**A**) GFP-tagged full-length (FL) Jmjd6 exclusively localizes in the nucleus of HeLa cells, with a small fraction associated with nucleolar structures (white arrows). (**B**) The C-terminal deletion Δ 363–403-Jmjd6–GFP displays a similar expression pattern as full-length Jmjd6. (**C**) The Δ 338–403-Jmjd6–GFP, lacking the polyS region, dramatically changes localization, with accumulation in distinct nucleoplasmic and nucleolar areas. (**D**) Replacing the polyS region (amino acids 340–365) with three alanine (A) residues (polySA-Jmjd6) resulted in a similar accumulation pattern. (**E**) Expression of the HA-tagged translational product of the Jmjd6 splice variant Hs3 [7] exhibiting an alternative C-terminus and lacking the polyS domain, detected with an anti-HA antibody. (**F**) C-terminal part of the amino acid sequence of wild-type Jmjd6, compared with the Jmjd6 splice variant Hs3.

Jmjd6 variants lacking the polyS domain are localized in the fibrillar centre of the nucleolus and in nuclear speckles

A C-terminally truncated $\Delta 363$ –403-Jmjd6–GFP variant, still containing the polyS domain, appears in a similar distribution as full-length Jmjd6 in the nuclei of HeLa cells (Figures 2A and 2B). However, a striking change in nuclear Jmjd6 distribution is observed after deletion of residues 338–403, including the polyS

region. PolyS-truncated Jmjd6 appears in distinct areas in the nucleoplasm with a significant amount in spots within the nucleolus (Figure 2C). A very similar pattern was obtained when we specifically deleted the polyS region from full-length Jmjd6 and replaced it with three alanine residues (PolySA-Jmjd6) (Figure 2D). Finally, we expressed the putative translational product of a splice variant of human Jmjd6 described in [7], which lacks the polyS domain (Figures 2E and 2F). The cDNA



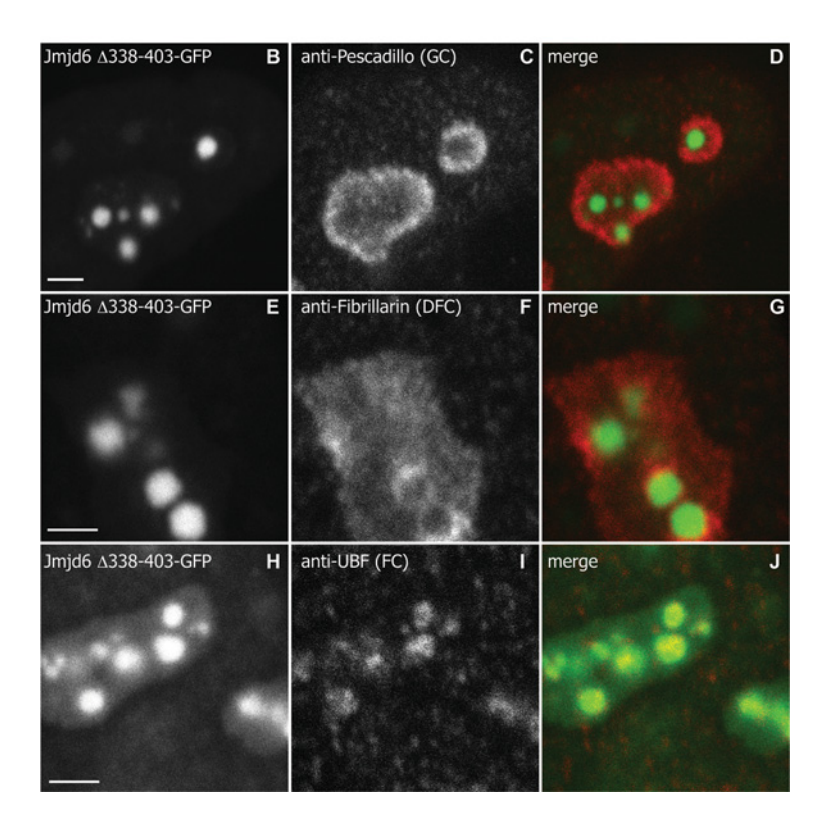


Figure 3 Jmjd6 lacking the polyS domain accumulates in the fibrillar centre of nucleoli

(A) Schematic drawing of a nucleolus and its subcompartments FC, DFC and GC. (B−J) Confocal sections of HeLa cells expressing a ∆338–403-Jmjd6–GFP mutant, which lacks the polyS domain and therefore accumulated in distinct nucleolar areas. Enlargements of nucleoli co-stained with antibodies against marker proteins for the nucleolar subcompartments GC (anti-pescadillo antibody), DFC (anti-fibrillarin) and FC (anti-UBF). (H−J) The accumulated Jmjd6 mutant is co-localized with anti-UBF staining in nucleoli, but not with (B−D) anti-pescadillo or (E−G) anti-fibrillarin counterstain. Scale bar, 2 μm.

for this splice variant was obtained after reverse transcription of HeLa cell mRNA. This protein localizes to nuclear speckles and the nucleolus in a similar manner to polySA-Jmjd6 (Figure 2E). Taken together, these results identify the polyS region as being, at least in part, responsible for the observed substantial changes in localization of Jmjd6. They also suggest that endogenous Jmjd6 in the nucleolus may be an alternatively spliced variant that lacks the polyS domain. This idea is supported by the failure of antibody ab10526 (C-terminal epitope residues 364–372) to recognize nucleolar Jmjd6.

Next, we analysed the sub-nucleolar localization of $\Delta 338$ –403-Jmjd6, lacking the polyS region. We used markers for three morphologically distinct nucleolar compartments; the FC (fibrillar centre) and the DFC (dense FC), which is embedded in the GC (granular centre) [32] (Figure 3A). We observed exclusion of $\Delta 338$ –403-Jmjd6-GFP from the GC, which was stained with an anti-Pescadillo antibody [33] and from the DFC, as stained with an anti-fibrillarin antibody [34] (Figures 3B–3G). In contrast, in the FC we observed co-localization of $\Delta 338$ –403-Jmjd6–GFP

with UBF (Figures 3H–3J) [34]. PolySA-Jmjd6 showed a similar distribution (Figure 4A). Its co-staining with UBF was maintained in mitosis, when it accumulates at distinct chromosomal sites, the NORs (nucleolar organizer regions) [35]. This was not observed for full-length Jmjd6–GFP (Figure 4A).

Jmjd6 lacking the polyS domain also accumulates in interchromatin granules, which we counterstained with the SC35 antibody (Figure 4B). These SC35-positive speckles are dispersed at the beginning of mitosis, and in metaphase they concentrate in one to three so-called MIGs (mitotic interchromatin granules) [36]. PolySA-Jmjd6 remains associated with these granules in metaphase; this association was not observed for full-length Jmjd6 (Figure 4B).

Jmjd6 shuttles between the nucleoplasm and the nucleolus

To investigate the kinetics of Jmjd6 shuttling between the nucleoplasm and nucleoli, we used fluorescence bleaching

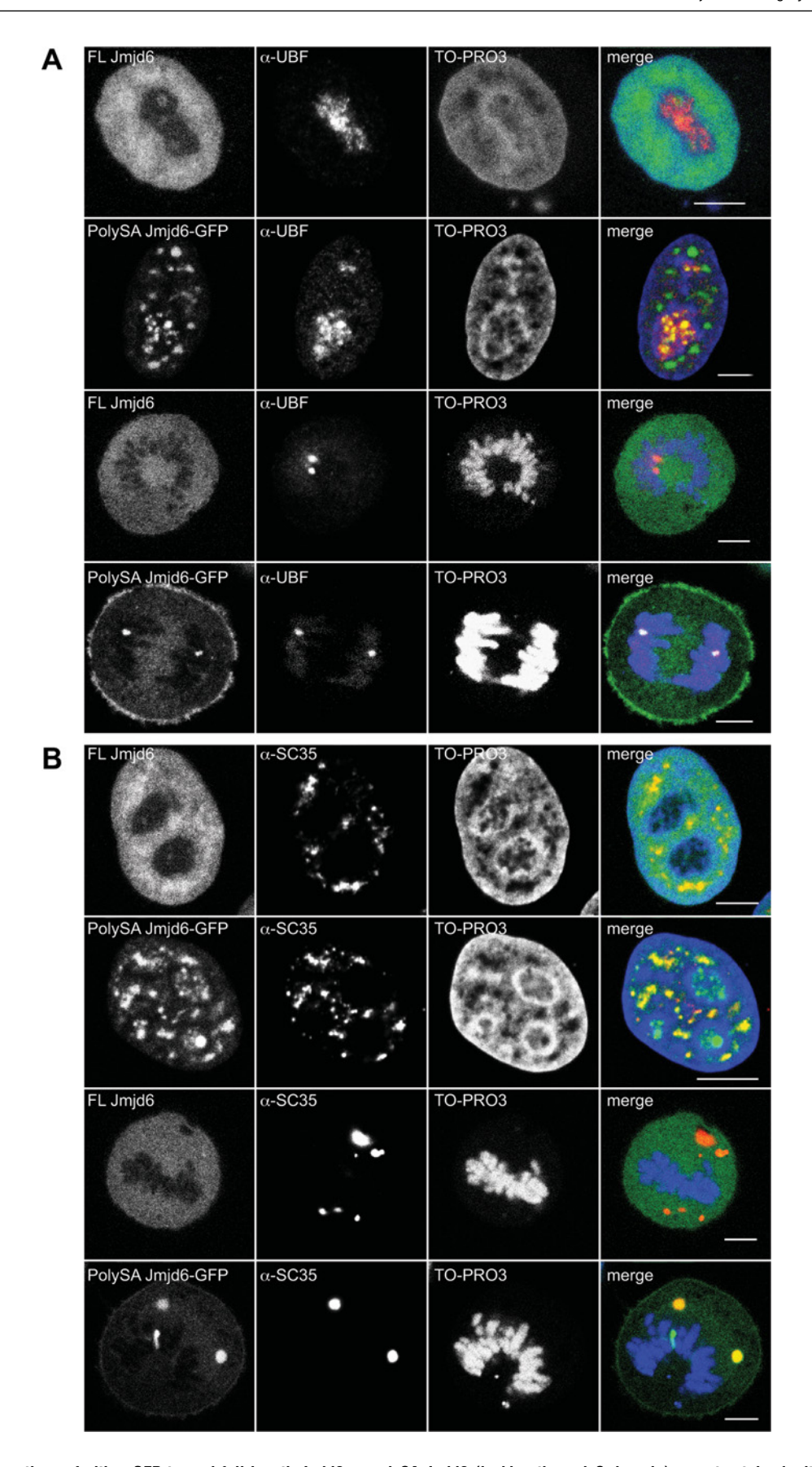


Figure 4 Confocal sections of either GFP-tagged full-length Jmjd6 or polySA-Jmjd6 (lacking the polyS domain), counterstained with either anti-UBF or anti-SC35 antibody

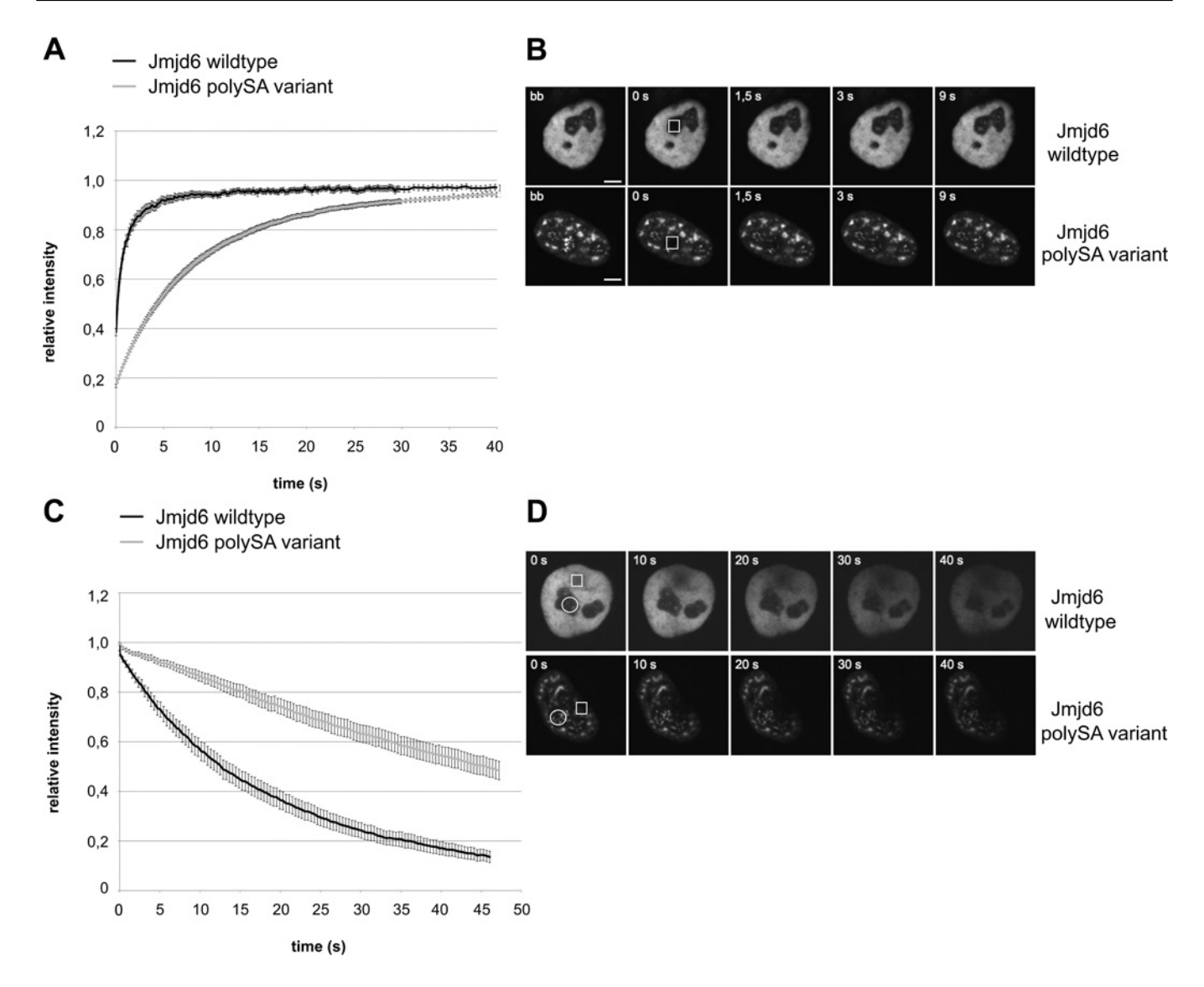


Figure 5 In vivo mobility measurements by FRAP and FLIP experiments of full-length Jmjd6 and the polySA-Jmjd6 variant

HeLa cells were transiently transfected with either GFP-tagged Jmjd6 or GFP-tagged polySA-Jmjd6 and analysed 24 h post-transfection. (**A**) Nucleolar shuttling kinetics of full-length Jmjd6 (black) and polySA-Jmjd6 (grey) after photobleaching the nucleolar fraction of either of the two proteins in FRAP experiments. The results are means \pm S.D. from 16 cells. (**B**) Representative confocal mid-sections from FRAP experiments. Boxes indicate the areas of bleaching. bb, before bleaching. (**C**) Fluorescence loss of nucleolar fractions of either Jmjd6 or polySA-Jmjd6 while repetitive bleaching of a nucleoplasmic fraction of the protein in a FLIP experiment. The results are the means \pm S.D. from nine cells. (**D**) Representative confocal mid-sections from FLIP experiments. Boxes represent areas of repetitive bleaching, circles represent areas of measurement.

coupled to live cell imaging. The results of FRAP and FLIP experiments indicate bidirectional shuttling of Jmjd6 between the nucleoplasm and nucleoli. After bleaching the nucleoli, full-length Jmjd6–GFP and polySA-Jmjd6–GFP were both recovered in the nucleoli. Recovery of full-length Jmjd6–GFP was complete within 10 s, with a half-life of $\sim\!2$ s. PolySA-Jmjd6–GFP was recovered within 30 s, with a half-life of 6 s (Figures 5A and 5B). When we constantly bleached a region in the nucleoplasm in FLIP experiments, we observed a decrease in fluorescence in the nucleolus, again in both cases (full-length and polySA-Jmjd6). A total of 50 % of polySA-Jmjd6–GFP fluorescence was lost within approximately 70 s, whereas Jmjd6–GFP fluorescence decreased

by 50% within 20 s (Figures 5C and 5D). These experiments indicate that both Jmjd6 and polySA-Jmjd6 shuttle rapidly between the nucleoplasm and the nucleolus. The association of the protein with the nucleolus appears stronger when the polyS domain is deleted.

Nucleolarly targeted Jmjd6 interacts predominantly with nucleolar proteins

Previous tandem-affinity purification and MS analysis of wildtype full-length Jmjd6 had revealed 39 interaction partners,

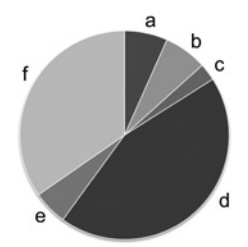
⁽A) The nucleolar fraction of the polySA-Jmjd6–GFP co-localizes with anti-UBF antibody staining in interphase nuclei and is therefore enriched in the fibrillar center of the nucleolus. This co-localization is maintained throughout mitosis, whereas the full-length (FL) Jmjd6 is evenly distributed throughout the cell in mitosis. (B) Transiently overexpressed GFP-tagged full-length Jmjd6 partially co-localizes with anti-SC35 staining in interphase HeLa nuclei, whereas the polySA-Jmjd6 accumulates in nucleoplasmic SC35-positive speckles. In mitosis, full-length Jmjd6 is evenly distributed throughout the cell. In contrast, the polySA-Jmjd6 co-localizes with MIGs. (A and B) DNA stained with TO-PR03. Scale bars, 5 μm.

A PolySA-Jmjd6-GFP

a b c d e

- a ribosomal 55% (65/118)
- b ribosome-associated 8% (9/118)
- nucleolar, non-ribosomal 4% (5/118)
- d RNA-processing 8% (9/118)
- e heatshock 3% (3/118)
- f miscellaneous 23% (27/118)

B Full-length Jmjd6-GFP



- a ribosomal 7% (5/75)
- b ribosome-associated 7% (5/75)
- c nucleolar, non-ribosomal 3% (2/75)
- d RNA-processing 44% (33/75)
- e heatshock 5% (4/75)
- f miscellaneous 35% (26/75)

C Protein overlap A and B

	acc no	name
а	P61247	40S ribosomal protein S3a
	P0CW22	40S ribosomal protein S17-like
	P62263	40S ribosomal protein S14
	P25398	40S ribosomal protein S12
b	O15372	Eukaryotic translation initiation factor 3 subunit H
	Q14152	Eukaryotic translation initiation factor 3 subunit A
	O15371	Eukaryotic translation initiation factor 3 subunit D
	Q99613	Eukaryotic translation initiation factor 3 subunit C
С	P06748	Nucleophosmin
	P19338	Nucleolin
d	Q8NC51	Plasminogen activator inhibitor 1 RNA-binding protein
	P26368	U2AF 65 kD
f	P50990	T-complex protein 1 subunit theta
	Q99832	T-complex protein 1 subunit eta
	P14174	Macrophage migration inhibitory factor
е	P11142	Heat shock cognate 71 kDa

Figure 6 Anti-GFP pulldown after transient overexpression of either full-length Jmjd6-GFP or polySA-Jmjd6-GFP in HEK-293T cells

After trypsinolysis, samples were analysed by LC-MS. (A) Pulldown of polySA-Jmjd6–GFP revealed 118 co-immunoprecipitated proteins. Out of these, 55 % were ribosomal proteins (65), whereas proteins involved in RNA processing accounted for only 8 % (9). (B) In the case of the full-length Jmjd6–GFP pulldown, 75 proteins were co-precipitated. From this, only 7 % (5) were ribosomal proteins, but 44 % (33) are involved in RNA processing. (C) List of the 16 proteins found in both pulldown experiments.

with 10% of the proteins being linked to the nucleolus [4]. In order to specifically analyse the nucleolar Jmjd6 interactome, we carried out a GFP-pulldown experiment with polySA-Jmjd6–GFP, coupled to proteomic analysis. As a result we identified 118 proteins as potential interaction partners of polySA-Jmjd6. Approximately 67% of those were associated with nucleolar function, including ribosomal and ribosome-associated proteins. In contrast, a pulldown with wild-type Jmjd6 delivered only $\sim\!15\%$ of proteins associated with the nucleolus, but $\sim\!45\%$ linked to RNA processing. The Jmjd6 substrate U2AF65 [4] was identified in both pulldowns (Figure 6).

These results demonstrate that a fraction of Jmjd6 is present in nucleoli, where they engage in protein interactions with other nucleolar proteins. Strikingly, the amount of nucleolar Jmjd6 was influenced dramatically by the presence/absence of the polyS domain.

Jmjd6 oligomerizes in vivo and in vitro

Previous work has suggested the formation of Jmjd6 oligomers in nuclear lysates from mammalian cells [20–22]. When we immunoprecipitated endogenous Jmjd6 from HeLa cells with an anti-Jmjd6 antibody and subjected it to SDS/PAGE and Western blotting, we observed, in addition to a band corresponding to monomeric Jmjd6 at 55 kDa, further bands corresponding to dimeric (120 kDa) and oligomeric (>170 kDa) forms (Figure 7A). Next, we tested full-length and various truncated and mutated Jmjd6 proteins for self-interaction in co-IP experiments. We subjected HEK-293T cells expressing GFP-tagged Jmjd6 and HA-tagged Jmjd6 to anti-GFP pulldown and SDS/PAGE and assayed for co-IP of Jmjd6–HA. Full-length Jmjd6, Δ338–403-Jmjd6 (lacking the polyS region), a mutant where the polyS region is replaced by three alanine residues (polySA-Jmjd6) and

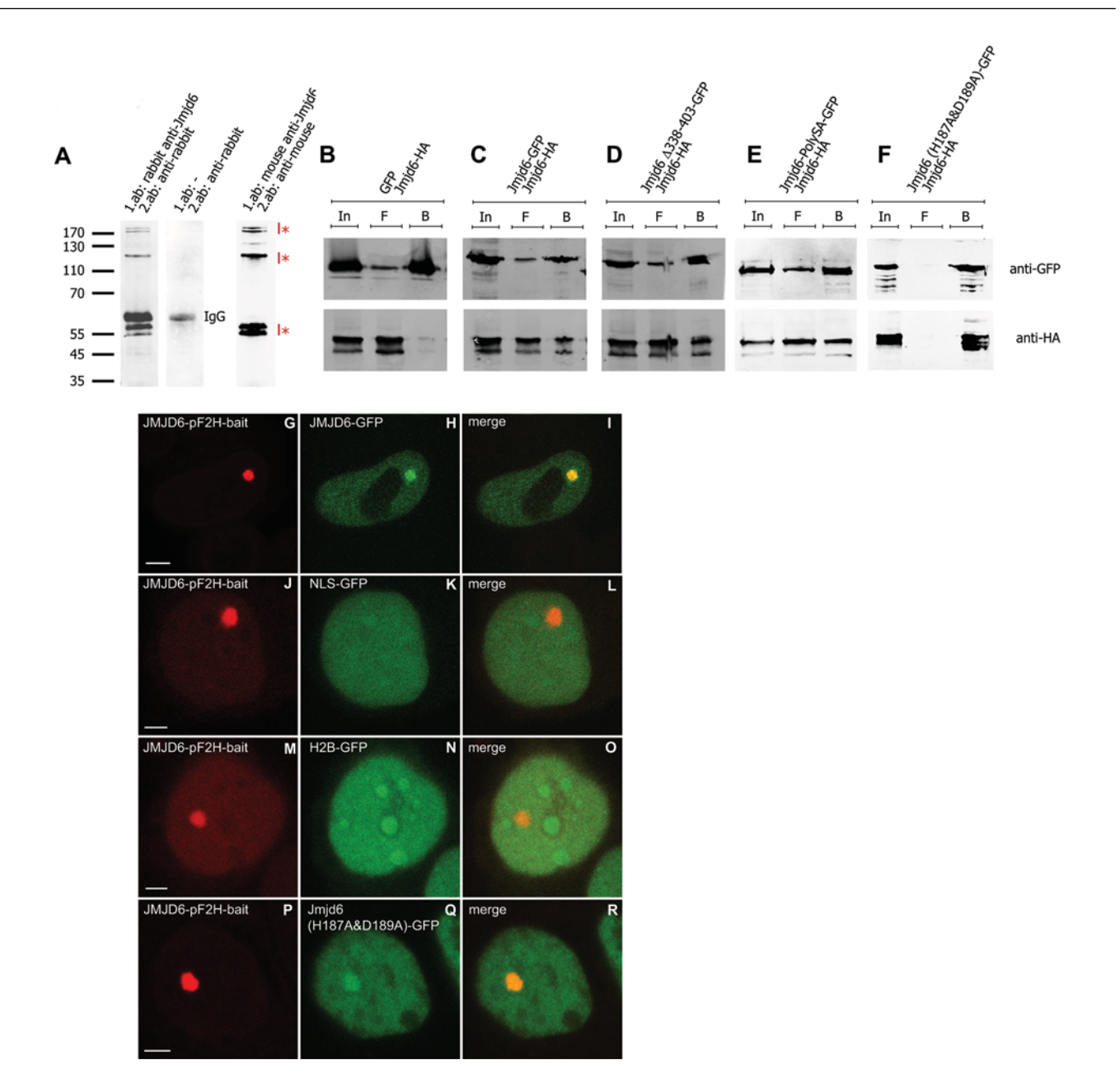


Figure 7 Jmjd6 oligomerizes in cells

(A) Immunoprecipitation of endogenous Jmjd6 from HeLa cells with a rabbit anti-Jmjd6 antibody (ab). Separation on SDS/PAGE and immunoblot revealed higher molecular mass bands with a rabbit anti-Jmjd6 antibody. Western blot without primary antibody and an anti-rabbit secondary antibody revealed the heavy chain (IgG) of the antibody used for immunoprecipitation. Western blot with a mouse anti-Jmjd6 antibody confirmed monomeric and higher molecular mass bands of endogenous Jmjd6 (indicated by red asterisks). Molecular markers are shown with masses in kDa. (B–F) Co-immunoprecipitation experiments after transient expression of GFP-tagged and HA-tagged Jmjd6 fusion proteins in HEK-293T cells and subsequent anti-GFP pulldown. Western blots with anti-GFP and anti-HA antibody show input (In), flow-through (F) and bead (B) fractions. (B) Pulldown of GFP-only does not co-purify HA-tagged Jmjd6, whereas (C) Jmjd6–GFP pulldown of GFP-the tested C-terminally truncated Jmjd6 variants and the enzymatically inactive Jmjd6 variant (H187A/D189A) still self-interact, similarly to full-length Jmjd6. B, beads; In, input; F, flow-through. (G–R) Expression of a triple fusion protein of Jmjd6, RFP and lac repressor (Jmjd6-pF2H-bait) in BHK cells. These cells exhibit a stable incorporation of several thousand copies of lac operator sequences. This results in accumulation of RFP-tagged Jmjd6 protein at the lac operator sequence site in the nucleus. Co-expression of GFP-fusion proteins shows interaction with full-length Jmjd6 (J–L), whereas Jmjd6 did not interact with GFP (coupled to an NLS) or (M–O) GFP-tagged Histone 2B. (P–R) An enzymatically inactive iron-binding Jmjd6 mutant (H187A and D189A) also displays oligomerization. Scale bar, 5 μm.

a catalytically inactive form of Jmjd6, Jmjd6 (H187A/D189A) [4], all bound to full-length Jmjd6 in such co-IP experiments (Figures 7B–7F). These results are in agreement with the proposal that two internal α -helical regions (residues 61–68 and 322–334) are responsible for Jmjd6 homodimerization, as predicted by crystallographic analysis [19].

To confirm that Jmjd6 interacts with itself *in vivo* we employed a F2H assay. For this, a Jmjd6–RFP–lac-repressor fusion protein is

tethered to a genomic region with stable incorporation of several thousand copies of the lac-operator sequence [26]. In the case of the interaction of Jmjd6–GFP with this fusion protein, RFP and GFP signals appear in the same spot. This assay reveals self-interaction both for full-length Jmjd6 and the enzymatically inactive Jmjd6 variant (H187A/D189A) (Figures 7G–7R).

In order to test whether oligomeric or monomeric Jmjd6 prevails in cell lysates, we combined native PAGE and SDS/PAGE

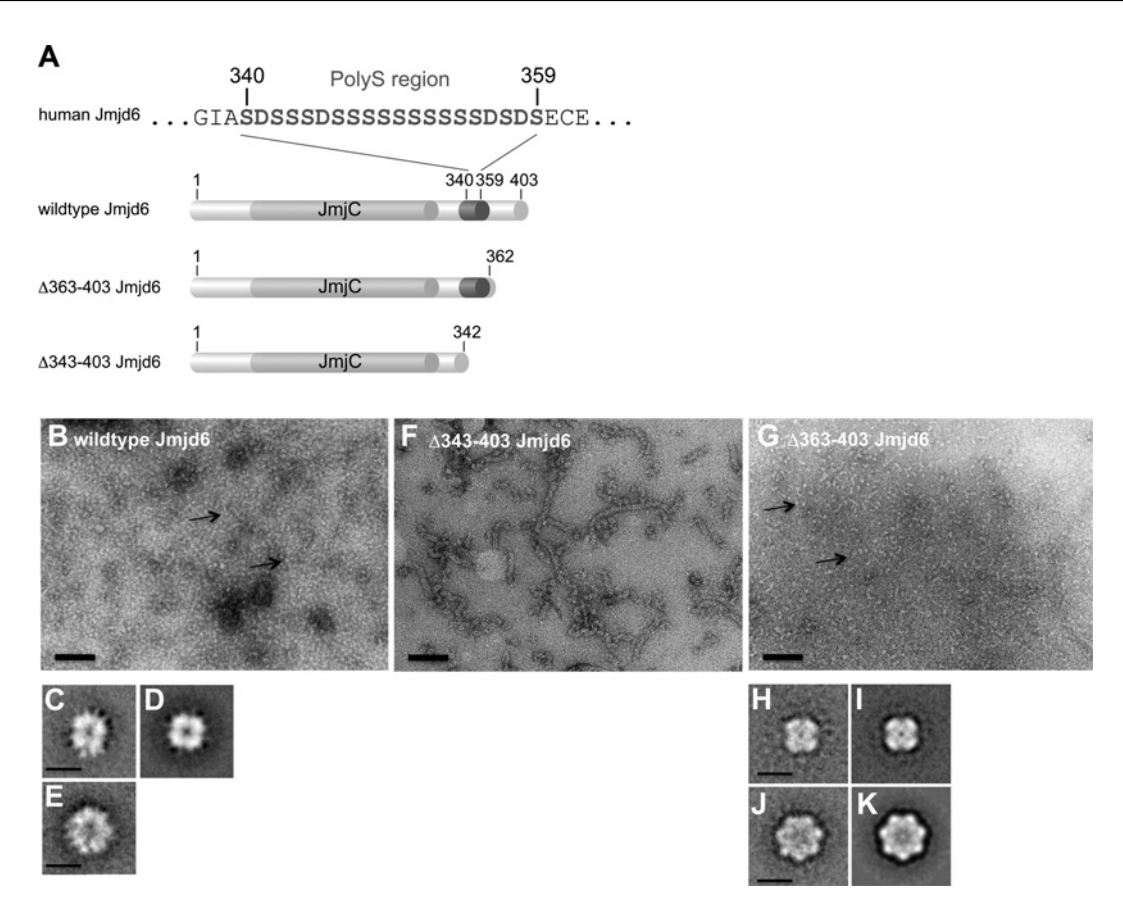


Figure 8 TEM of recombinant full-length and C-terminally truncated Jmjd6

(A) Cartoon representation of the Jmjd6 domain structure showing the JmjC domain (light grey) and the polyS region (dark grey) with 16 consecutive serine residues interrupted by four aspartate residues. (B) Electron micrograph of negatively stained full-length Jmjd6 exhibiting a ring-like structure. ($\mathbf{C}-\mathbf{E}$) Two classes selected from the classification. (D) Same as (C), but four-fold symmetry has been applied. (F) Electron micrograph of negatively stained $\triangle 338-403$ -Jmjd6 construct, lacking the polyS region and assembling in fibrils. (G) Electron micrograph of negatively stained $\triangle 363-403$ -Jmjd6 construct, with polyS region also exhibiting a ring-like structure resembling the full-length protein. ($\mathbf{H}-\mathbf{K}$) Two selected classes from $\triangle 363-403$ -Jmjd6. (I) Same as (H), but with four-fold symmetry imposed. (K) Same as (J), but with a seven-fold symmetry applied. Scale bars, (B, F and G) 100 nm; ($\mathbf{C}-\mathbf{E}$ and $\mathbf{H}-\mathbf{K}$) 100 Å.

in a 2D-separation of HA-tagged Jmjd6 from HEK-293T cells. Native PAGE resulted in two distinct Jmjd6 bands (Supplementary Figure S1A at http://www.biochemj.org/bj/453/bj4530357add.htm). Subsequent separation of these Jmjd6 species on SDS/PAGE, without denaturing the samples, reveals high-molecular-mass Jmjd6 forms (Supplementary Figure S1C). In contrast, denaturing the samples before SDS/PAGE resulted in mainly monomeric Jmjd6 (Supplementary Figure S1D). These data indicate that oligomeric forms of Jmjd6 exist in cells and that these oligomers are most likely not irreversibly covalently linked.

BIFC assays visualize protein–protein interactions within cells in the subcellular structures where they occur [30]. When applied to Jmjd6 fused to either of two halves of YFP, we found a strong YFP signal in the nucleus, again supporting self-interaction of Jmjd6 in the nucleoplasm (Supplementary Figure S2 at http://www.biochemj.org/bj/453/bj4530357add.htm). In addition, a BIFC signal was observed in the nucleolus, suggesting a nucleolar localization of oligomeric Jmjd6.

Jmjd6 oligomer structure depends on the presence of the polyS

Initial analytical SEC analysis predicted that purified recombinant full-length His-tagged human Jmjd6 protein formed higher molecular mass species (results not shown). In order to obtain

higher resolution information on Jmjd6 oligomers, we performed TEM. Full-length and two C-terminally truncated His-tagged Jmjd6 versions ($\Delta 343$ –403-Jmjd6, lacking the polyS region and Δ363–403-Jmid6, including the polyS region but lacking the C-terminus) (Figure 8A), were expressed in and purified from E. coli and analysed by negative staining. Full-length Jmjd6 was observed to form rings as shown in the TEM micrographs (Figures 8B–8E). For image analysis, 3122 particles were selected which were distributed into groups of 10 and 30 classes. Two interesting classes were analysed; a tetramer of dimers with a diameter of 117 ± 15 Å to which four-fold symmetry was imposed (Figures 8C and 8D) and a class forming a higher oligomeric ring (Figure 8E) with a diameter of 161 ± 15 Å (symmetry difficult to establish). In contrast, the C-terminally truncated His- $\Delta 343$ -403-Jmjd6 construct lacking the polyS region showed formation of filament-like structures (as shown in Figure 8F). Aligning the images in order to identify common features among these filaments (results not shown) suggested that there is no clear organization of the protein inside these filaments. TEM analysis of His- $\Delta 363$ -403-Jmjd6, which includes the polyS domain, showed that this again formed oligomeric rings (Figures 8G-8K). Image analysis was carried out by aligning 4194 particles and classifying them into 10–30 classes. This showed that oligomers of $\Delta 363$ – 403-Jmjd6 probably exist in two classes: a tetramer of dimers 116 ± 15 Å (Figures 8H and 8I) and a heptamer of dimers with a diameter of approximately 153 ± 15 Å (Figures 8J and 8K).

In summary, these TEM data reveal that $\Delta 343$ –403-Jmjd6 lacking the polyS domain forms filamentous structures, whereas Jmjd6 versions with an intact polyS domain form oligomers with ring morphology. Thus the polyS domain is either necessary for the formation of Jmjd6 oligomer rings or it blocks filament formation. Overall, the results clearly demonstrate that the polyS domain can have a regulatory influence on the oligomeric structure of Jmjd6 *in vitro*.

DISCUSSION

The Fe(II)- and 2OG-dependent oxygenase Jmjd6 has been proposed to play important functions in splicing [2,4], due in part to its ability to hydroxylate lysine residues in U2AF65. In the present study we demonstrate that Jmjd6 may also have a function in the nucleolus. A version of Jmjd6 which is enriched in the nucleus has been found to interact with nucleolar proteins. These were mainly ribosomal proteins; however, multiple proteins involved in rRNA processing were also present. It is possible that due to the strong interaction of ribosomal proteins with rRNA, the bulk of precipitated proteins did not directly interact with Jmjd6. However, a nucleolar function of Jmjd6 is also suggested by its specific localization in the FC of the nucleolus, where transcription of rDNA by RNA polymerase I takes place [34]. FRAP and FLIP analyses reveal that shuttling of Jmjd6 between nucleoli and nucleoplasm is rapid as described for other proteins involved in rRNA transcription and processing. In contrast, ribosomal proteins move much slower in and out of the nucleolus [37,38]. These results suggest functional association of Jmjd6 with the RNA processing machinery in the nucleolus. Pre-rRNA transcripts are spliced and matured by snoRNPs (small nucleolar ribonucleoproteins) [34]. Several SR (serine-arginine)rich proteins, for instance the Jmjd6 substrate U2AF65, are also reported to be present in the nucleolus [39]. However, owing to the co-localization with the transcription factor UBF and because for some other 2OG oxygenases multiple protein substrates have been described [40], it is also possible that Jmjd6 has other non-splicing-associated substrates in the nucleolus. It is notable that recently two other human 2OG oxygenases with a preferred nucleolar localization have been reported to hydroxylate ribosomal proteins [41].

In accordance with the Jmjd6 crystal structure proposing two internal α -helices as an interface for dimerization [19] several lines of evidence support the idea that Jmjd6 forms oligomers or at least dimers in cells. Oligomerization was demonstrated both for the wild-type Jmjd6 as well as the C-terminally deleted mutations lacking the polyS domain. In the BIFC assay, Jmjd6 interaction with itself was seen in both the nucleoplasm and in the nucleolus. Jmjd6 has been shown to self-hydroxylate two internal lysine residues, Lys¹¹¹ and Lys¹⁶⁷ [42]. In our experiments, interaction of Jmjd6 with itself and ring formation *in vitro* were also possible with active site mutants of Jmjd6, indicating that self-hydroxylation of Jmjd6 was not required. However, both Lys¹¹¹ and Lys¹⁶⁷ are part of a flexible loop and therefore might be involved in regulating the stability of an oligomeric structure.

The observed ring-like structures of Jmjd6 display similarity with protein complexes involved in RNA metabolism. Proteins adapting such ring structures include the exosome complex and the SM and LSM (SM-like) protein families [43]. Human SM proteins build a heteroheptameric ring-like complex, which binds to a conserved site found in single-stranded regions of snRNAs (small nuclear RNAs) [44,45]. The SM ring is established around the RNA molecule in the cytoplasm via a dedicated pathway, and then transferred to the nucleus to act at the centre of snRNPs

in pre-mRNA splicing [46]. A direct interaction with RNA occurs through RNA-binding sites within flexible loops facing the central pore of the SM ring [47]. LSM proteins also form heteroheptameric rings, but can assemble in the absence of RNA molecules [48]. The LSM rings bind, also via the central pore, to U6 snRNA [48]. Jmjd6 forms homo-oligomeric rings without the obvious presence of RNA. However, experimental evidence suggests that Jmjd6 interacts with RNA; Hong et al. [10] reported binding of a random 27 nt single-stranded RNA molecule to recombinant full-length Jmjd6 in EMSAs. The size of the central pore in wild-type Jmjd6 rings is approximately 10–18 Å and thus would allow passage of ssRNA.

The results of the present study suggest that alternative splicing of the Jmjd6 pre-mRNA may at least in part contribute to enrichment of Jmjd6 in the nucleolus. The fact that the antibody ab10526 fails to recognize the bulk of nucleolar Jmjd6 stained with two other anti-Jmjd6 antibodies indicates that its C-terminal epitope (residues 364–372 [20]) could be missing from nucleolar Jmjd6. Alternatively spliced versions of Jmjd6 exist in mouse tissue and are predicted to occur in humans [7]. We confirmed that HeLa cells express a version of Jmjd6 where the alternative exon 5 is included and a polyadenylation signal in intron 7 is used. This changes the reading frame of exon 6 leading to translation of a C-terminal sequence without a polyS domain (Figure 2F). When ectopically expressed in HeLa cells this translation product was found in nuclear speckles and in the nucleolus.

On the other hand, full-length Jmjd6 can also be found in the nucleolus. Use of ab10526 consistently reveals a weak signal in the nucleolus and a small proportion of full-length Jmjd6–GFP can also be found in the nucleolus. Moreover, our FLIP and FRAP experiments reveal that full-length Jmjd6 shuttles between the nucleolus and the nucleoplasm. To what extent this involves the polyS domain, including via post-translational modifications, requires further investigation.

The polyS domain in Jmjd6 is highly conserved in the animal kingdom. A previous study identified 59 proteins with polyS regions in the human genome; it is proposed that replicative slippage at the DNA level was most likely responsible for their facile evolution [8]. In the case of Jmjd6, clear evidence for evolutionary selection of the polyS domain was presented [8]. This conclusion suggests that the function, and related structure, of the Jmjd6 polyS domain are probably also conserved. It is unclear if our proposed role for the polyS region of Jmjd6 applies to other polyS-containing proteins; however, SRrp37 possesses a polyS domain and has a dual localization in nuclear speckles and in the nucleolus [12]. On the other hand, deletion of the polyS region in the RNPS1 protein did not result in an obvious change in localization after overexpression in HeLa cells [13]. Moreover, 30 consecutive serine residues fused to YFP did not display a specific localization pattern in COS-7 cells [49].

The importance of the polyS domain of Jmjd6 for both oligomeric structure and nuclear/nucleolar shuttling is striking. We propose that the substantial differences in structure are functionally related to the dramatically different behaviours of Jmjd6 variants with or without polyS domains within the nucleus.

AUTHOR CONTRIBUTION

Alexander Wolf, Monica Mantri, Catherine Vénien-Bryan, Heinrich Leonhardt, Benedikt Kessler, Christopher Schofield and Angelika Böttger designed the research and analysed experiments. Alexander Wolf, Monica Mantri, Christopher Schofield and Angelika Böttger wrote the paper. Alexander Wolf and Astrid Heim performed immunoprecipitation, F2H assay and immunofluorescence analysis. Monica Mantri purified and analysed recombinant proteins. Gregory Dadie and Catherine Vénien-Bryan performed TEM analysis. Mukram Mackeen and Benedikt Kessler performed MS analysis. Udo Müller

and Lothar Schermelleh performed super-resolution imaging. Erika Fichter and Lothar Schermelleh analysed FRAP/FLIP data.

ACKNOWLEDGEMENTS

We thank Katrin Schneider and Andreas Maiser for technical help and advice. We thank Dirk Eick (Research Unit Molecular Epigenetics, Helmholtz Zentrum München, German Research Center for Environmental Health, Munich, Germany) for providing the anti-Pescadillo antibody. BIFC plasmids were a gift from Tom Kerppola (Department of Biological Chemistry, University of Michigan School of Medicine, Ann Arbor, MI, U.S.A.).

FUNDING

This work was supported by the Biotechnology and Biological Research Council, the Wellcome Trust and by the Deutsche Forschungsgemeinschaft [grant numbers B01748-3 and B01748-6]. A.W. was a recipient of an EMBO long-term fellowship.

REFERENCES

- 1 Wolf, A., Schmitz, C. and Bottger, A. (2007) Changing story of the receptor for phosphatidylserine-dependent clearance of apoptotic cells. EMBO Rep. 8, 465–469
- 2 Boeckel, J. N., Guarani, V., Koyanagi, M., Roexe, T., Lengeling, A., Schermuly, R. T., Gellert, P., Braun, T., Zeiher, A. and Dimmeler, S. (2011) Jumonji domain-containing protein 6 (Jmjd6) is required for angiogenic sprouting and regulates splicing of VEGF-receptor 1. Proc. Natl. Acad. Sci. U.S.A. **108**, 3276–3281
- 3 Mantri, M., Loik, N. D., Hamed, R. B., Claridge, T. D., McCullagh, J. S. and Schofield, C. J. (2011) The 2-oxoglutarate-dependent oxygenase JMJD6 catalyses oxidation of lysine residues to give 5S-hydroxylysine residues. ChemBioChem. 12, 531–534
- 4 Webby, C. J., Wolf, A., Gromak, N., Dreger, M., Kramer, H., Kessler, B., Nielsen, M. L., Schmitz, C., Butler, D. S., Yates, 3rd, J. R. et al. (2009) Jmjd6 catalyses lysyl-hydroxylation of U2AF65, a protein associated with RNA splicing. Science 325, 00_03
- 5 Unoki, M., Masuda, A., Dohmae, N., Arita, K., Yoshimatsu, M., Iwai, Y., Fukui, Y., Ueda, K., Hamamoto, R., Shirakawa, M. et al. (2013) Lysyl 5-hydroxylation, a novel histone modification, by Jumonji domain containing 6 (JMJD6). J. Biol. Chem. 288, 6053–6062
- 6 Cikala, M., Alexandrova, O., David, C. N., Proschel, M., Stiening, B., Cramer, P. and Bottger, A. (2004) The phosphatidylserine receptor from Hydra is a nuclear protein with potential Fe(II) dependent oxygenase activity. BMC Cell Biol. 5, 26
- 7 Hahn, P., Bose, J., Edler, S. and Lengeling, A. (2008) Genomic structure and expression of Jmjd6 and evolutionary analysis in the context of related JmjC domain containing proteins. BMC Genomics 9, 293
- Huntley, M. A. and Golding, G. B. (2006) Selection and slippage creating serine homopolymers. Mol. Biol. Evol. 23, 2017–2025
- 9 Dunker, A. K., Brown, C. J., Lawson, J. D., lakoucheva, L. M. and Obradovic, Z. (2002) Intrinsic disorder and protein function. Biochemistry 41, 6573–6582
- 10 Hong, X., Zang, J., White, J., Wang, C., Pan, C. H., Zhao, R., Murphy, R. C., Dai, S., Henson, P., Kappler, J. W. et al. (2010) Interaction of JMJD6 with single-stranded RNA. Proc. Natl. Acad. Sci. U.S.A. 107, 14568–14572
- Howard, M. B., Ekborg, N. A., Taylor, L. E., Hutcheson, S. W. and Weiner, R. M. (2004) Identification and analysis of polyserine linker domains in prokaryotic proteins with emphasis on the marine bacterium *Microbulbifer degradans*. Protein Sci. 13, 1422–1425
- 12 Ouyang, P. (2009) SRrp37, a novel splicing regulator located in the nuclear speckles and nucleoli, interacts with SC35 and modulates alternative pre-mRNA splicing in vivo. J. Cell. Biochem. 108, 304–314
- 13 Sakashita, E., Tatsumi, S., Werner, D., Endo, H. and Mayeda, A. (2004) Human RNPS1 and its associated factors: a versatile alternative pre-mRNA splicing regulator in vivo. Mol. Cell. Biol. 24, 1174–1187
- 14 Lando, D., Peet, D. J., Gorman, J. J., Whelan, D. A., Whitelaw, M. L. and Bruick, R. K. (2002) FIH-1 is an asparaginyl hydroxylase enzyme that regulates the transcriptional activity of hypoxia-inducible factor. Genes Dev. 16, 1466–1471
- 15 Elkins, J. M., Hewitson, K. S., McNeill, L. A., Seibel, J. F., Schlemminger, I., Pugh, C. W., Ratcliffe, P. J. and Schofield, C. J. (2003) Structure of factor-inhibiting hypoxia-inducible factor (HIF) reveals mechanism of oxidative modification of HIF-1α. J. Biol. Chem. 278, 1802–1806
- 16 Lancaster, D. E., McNeill, L. A., McDonough, M. A., Aplin, R. T., Hewitson, K. S., Pugh, C. W., Ratcliffe, P. J. and Schofield, C. J. (2004) Disruption of dimerization and substrate phosphorylation inhibit factor inhibiting hypoxia-inducible factor (FIH) activity. Biochem. J. 383, 429–437
- 17 Clifton, I. J., McDonough, M. A., Ehrismann, D., Kershaw, N. J., Granatino, N. and Schofield, C. J. (2006) Structural studies on 2-oxoglutarate oxygenases and related double-stranded β-helix fold proteins. J. Inorg. Biochem. 100, 644–669

- 18 Woo, E.-J., Dunwell, J. M., Goodenough, P. W., Marvier, A. C. and Pickersgill, R. W. (2000) Germin is a manganese containing homohexamer with oxalate oxidase and superoxide dismutase activities. Nat. Struct. Mol. Biol. 7, 1036–1040
- 19 Mantri, M., Krojer, T., Bagg, E. A., Webby, C. J., Butler, D. S., Kochan, G., Kavanagh, K. L., Oppermann, U., McDonough, M. A. and Schofield, C. J. (2010) Crystal structure of the 2-oxoglutarate- and Fe(II)-dependent lysyl hydroxylase JMJD6. J. Mol. Biol. 401, 211–222
- 20 Hahn, P., Wegener, I., Burrells, A., Bose, J., Wolf, A., Erck, C., Butler, D., Schofield, C. J., Bottger, A. and Lengeling, A. (2010) Analysis of Jmjd6 cellular localization and testing for its involvement in histone demethylation. PLoS ONE 5, e13769
- 21 Han, G., Li, J., Wang, Y., Li, X., Mao, H., Liu, Y. and Chen, C. D. (2012) The hydroxylation activity of Jmjd6 is required for its homo-oligomerization. J. Cell. Biochem. 113, 1663–1670
- 22 Tibrewal, N., Liu, T., Li, H. and Birge, R. B. (2007) Characterization of the biochemical and biophysical properties of the phosphatidylserine receptor (PS-R) gene product. Mol. Cell. Biochem. 304, 119–125
- 23 Frank, J., Radermacher, M., Penczek, P., Zhu, J., Li, Y., Ladjadj, M. and Leith, A. (1996) SPIDER and WEB: processing and visualization of images in 3D electron microscopy and related fields. J. Struct. Biol. **116**, 190–199
- 24 Frank, J. (1990) Classification of macromolecular assemblies studied as 'single particles'. Q. Rev. Biophys. 23, 281–329
- 25 Tsukamoto, T., Hashiguchi, N., Janicki, S. M., Tumbar, T., Belmont, A. S. and Spector, D. L. (2000) Visualization of gene activity in living cells. Nat. Cell Biol. 2, 871–878
- 26 Zolghadr, K., Mortusewicz, O., Rothbauer, U., Kleinhans, R., Goehler, H., Wanker, E. E., Cardoso, M. C. and Leonhardt, H. (2008) A fluorescent two-hybrid assay for direct visualization of protein interactions in living cells. Mol. Cell. Proteomics 7, 2279–2287
- 27 Mackeen, M. M., Kramer, H. B., Chang, K. H., Coleman, M. L., Hopkinson, R. J., Schofield, C. J. and Kessler, B. M. (2010) Small-molecule-based inhibition of histone demethylation in cells assessed by quantitative mass spectrometry. J. Proteome Res. 9, 4082–4092
- 28 Taylor, G. K. and Goodlett, D. R. (2005) Rules governing protein identification by mass spectrometry. Rapid Commun. Mass Spectrom. 19, 3420
- 29 Schermelleh, L., Haemmer, A., Spada, F., Rosing, N., Meilinger, D., Rothbauer, U., Cardoso, M. C. and Leonhardt, H. (2007) Dynamics of Dnmt1 interaction with the replication machinery and its role in postreplicative maintenance of DNA methylation. Nucleic Acids Res. 35, 4301–4312
- Hu, C. D. and Kerppola, T. K. (2003) Simultaneous visualization of multiple protein interactions in living cells using multicolor fluorescence complementation analysis. Nat. Biotechnol. 21, 539–545
- 31 Schermelleh, L., Carlton, P. M., Haase, S., Shao, L., Winoto, L., Kner, P., Burke, B., Cardoso, M. C., Agard, D. A., Gustafsson, M. G. et al. (2008) Subdiffraction multicolor imaging of the nuclear periphery with 3D structured illumination microscopy. Science 320, 1332–1336
- 32 Sirri, V., Urcuqui-Inchima, S., Roussel, P. and Hernandez-Verdun, D. (2008) Nucleolus: the fascinating nuclear body. Histochem. Cell Biol. 129, 13–31
- 33 Holzel, M., Grimm, T., Rohrmoser, M., Malamoussi, A., Harasim, T., Gruber-Eber, A., Kremmer, E. and Eick, D. (2007) The BRCT domain of mammalian Pes1 is crucial for nucleolar localization and rRNA processing. Nucleic Acids Res. 35, 789–800
- 34 Boisvert, F. M., van Koningsbruggen, S., Navascues, J. and Lamond, A. I. (2007) The multifunctional nucleolus. Nat. Rev. Mol. Cell Biol. 8, 574–585
- 35 Hernandez-Verdun, D. (2011) Assembly and disassembly of the nucleolus during the cell cycle. Nucleus 2, 189–194
- 36 Ferreira, J. A., Carmo-Fonseca, M. and Lamond, A. I. (1994) Differential interaction of splicing snRNPs with coiled bodies and interchromatin granules during mitosis and assembly of daughter cell nuclei. J. Cell Biol. 126, 11–23
- 37 Chen, D. and Huang, S. (2001) Nucleolar components involved in ribosome biogenesis cycle between the nucleolus and nucleoplasm in interphase cells. J. Cell Biol. 153, 169–176
- 38 Phair, R. D. and Misteli, T. (2000) High mobility of proteins in the mammalian cell nucleus. Nature 404, 604–609
- 39 Leung, A. K., Trinkle-Mulcahy, L., Lam, Y. W., Andersen, J. S., Mann, M. and Lamond, A. I. (2006) NOPdb: Nucleolar Proteome Database. Nucleic Acids Res. 34, D218–D220
- 40 Loenarz, C. and Schofield, C. J. (2011) Physiological and biochemical aspects of hydroxylations and demethylations catalyzed by human 2-oxoglutarate oxygenases. Trends Biochem. Sci. 36, 7–18
- 41 Ge, W., Wolf, A., Feng, T., Ho, C. H., Sekirnik, R., Zayer, A., Granatino, N., Cockman, M. E., Loenarz, C., Loik, N. D. et al. (2012) Oxygenase-catalyzed ribosome hydroxylation occurs in prokaryotes and humans. Nat. Chem. Biol. 8, 960–962
- 42 Mantri, M., Webby, C. J., Loik, N. D., Hamed, R. B., Nielsen, M. L., McDonough, M. A., McCullagh, J. S. O., Bottger, A., Schofield, C. J. and Wolf, A. (2012) Self-hydroxylation of the splicing factor lysyl hydroxylase, JMJD6. Med. Chem. Commum. 3, 80–85

- 43 Pruijn, G. J. (2005) Doughnuts dealing with RNA. Nat. Struct. Mol. Biol. 12, 562–564
- 44 Liautard, J. P., Sri-Widada, J., Brunel, C. and Jeanteur, P. (1982) Structural organization of ribonucleoproteins containing small nuclear RNAs from HeLa cells. Proteins interact closely with a similar structural domain of U1, U2, U4 and U5 small nuclear RNAs. J. Mol. Biol. 162, 623–643
- 45 Urlaub, H., Raker, V. A., Kostka, S. and Luhrmann, R. (2001) Sm protein-Sm site RNA interactions within the inner ring of the spliceosomal snRNP core structure. EMBO J. 20, 187–196
- 46 Meister, G., Eggert, C. and Fischer, U. (2002) SMN-mediated assembly of RNPs: a complex story. Trends Cell Biol. 12, 472–478

Received 12 April 2013/14 May 2013; accepted 21 May 2013 Published as BJ Immediate Publication 21 May 2013, doi:10.1042/BJ20130529

- 47 Kambach, C., Walke, S., Young, R., Avis, J. M., de la Fortelle, E., Raker, V. A., Luhrmann, R., Li, J. and Nagai, K. (1999) Crystal structures of two Sm protein complexes and their implications for the assembly of the spliceosomal snRNPs. Cell 96, 375–387
- 48 Achsel, T., Brahms, H., Kastner, B., Bachi, A., Wilm, M. and Luhrmann, R. (1999) A doughnut-shaped heteromer of human Sm-like proteins binds to the 3'-end of U6 snRNA, thereby facilitating U4/U6 duplex formation in vitro. EMBO J. 18, 5789–5802
- 49 Oma, Y., Kino, Y., Sasagawa, N. and Ishiura, S. (2004) Intracellular localization of homopolymeric amino acid-containing proteins expressed in mammalian cells. J. Biol. Chem. 279, 21217–21222



SUPPLEMENTARY ONLINE DATA

The polyserine domain of the lysyl-5 hydroxylase Jmjd6 mediates subnuclear localization

Alexander WOLF*1, Monica MANTRI†1, Astrid HEIM‡, Udo MÜLLER‡, Erika FICHTER‡, Mukram M. MACKEEN†2, Lothar SCHERMELLEH‡§, Gregory DADIE||, Heinrich LEONHARDT‡, Catherine VÉNIEN-BRYAN||, Benedikt M. KESSLER¶, Christopher J. SCHOFIELD†1,3 and Angelika BÖTTGER‡1,3

*Institute of Molecular Toxicology and Pharmacology, Helmholtz Zentrum München-German Research Center for Environmental Health, Ingolstädter Landstrasse 1, 85764 Neuherberg, Germany, †Chemistry Research Laboratory and Oxford Centre for Integrative Systems Biology, University of Oxford, 12 Mansfield Road, Oxford OX1 3TA, U.K., ‡Department of Biology II, Ludwig Maximilians University, Munich, Grosshaderner Strasse 2, 82152 Planegg-Martinsried, Germany, §Department of Biochemistry, University of Oxford, South Parks Road, Oxford OX1 3QU, U.K., ||IMPMC, UMR7590, CNRS, Université Pierre et Marie Curie, Case 115, 4 place Jussieu, 75252 Paris Cedex 05, France, and ¶Henry Wellcome Building for Molecular Physiology, Nuffield Department of Medicine, University of Oxford, Oxford OX3 7BN, U.K.

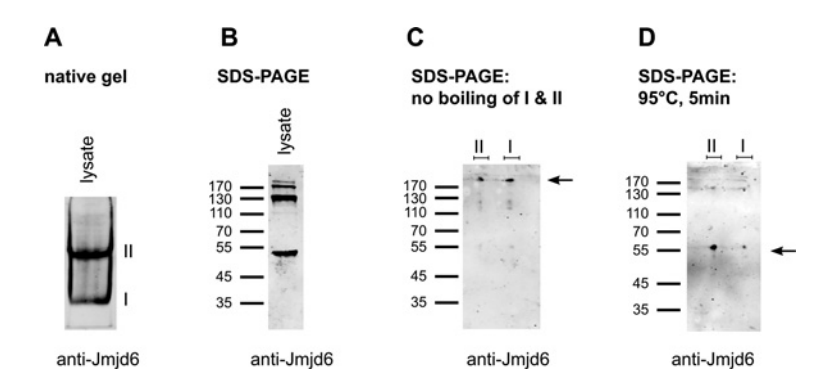


Figure S1 The multimeric state of Jmjd6

(A) Lysate of HEK-293T cells overexpressing HA-tagged Jmjd6 was loaded on a non-denaturing native gel. Western blotting and staining with an anti-Jmjd6 antibody revealed two distinct Jmjd6 bands (I and II). (B) Lysate of HEK-293T cells overexpressing HA-tagged Jmjd6 was loaded on to a standard SDS/PAGE (12% gel). Western blotting and staining with an anti-Jmjd6 antibody revealed a monomeric band at approximately 55 kDa and several higher molecular mass bands. (C) Native gel bands I and II were cut-out and separated by putting on top of a SDS/PAGE gel without previous denaturing steps. Western blotting and staining with an anti-Jmjd6 antibody revealed mainly multimeric Jmdj6 species (black arrow in C). (D) Denaturing native gel bands I and II by boiling in SDS/PAGE loading buffer (5 min on 95 °C) prior to loading on to SDS/PAGE resulted in disruption of the multimeric Jmjd6 complex and gave mainly monomeric Jmjd6 species (black arrow in D). Molecular masses in kDa are indicated.

¹ These authors contributed equally to this work.

² Present address: School of Chemical Science, Faculty of Science and Technology, Universiti Kebangsaan Malaysia, 43600 Bangi, Selangor Darul Ehsan, Malaysia.

³ Correspondence may be addressed to either of these authors (email christopher.schofield@chem.ox.ac.uk or boettger@zi.biologie.uni-muenchen.de).

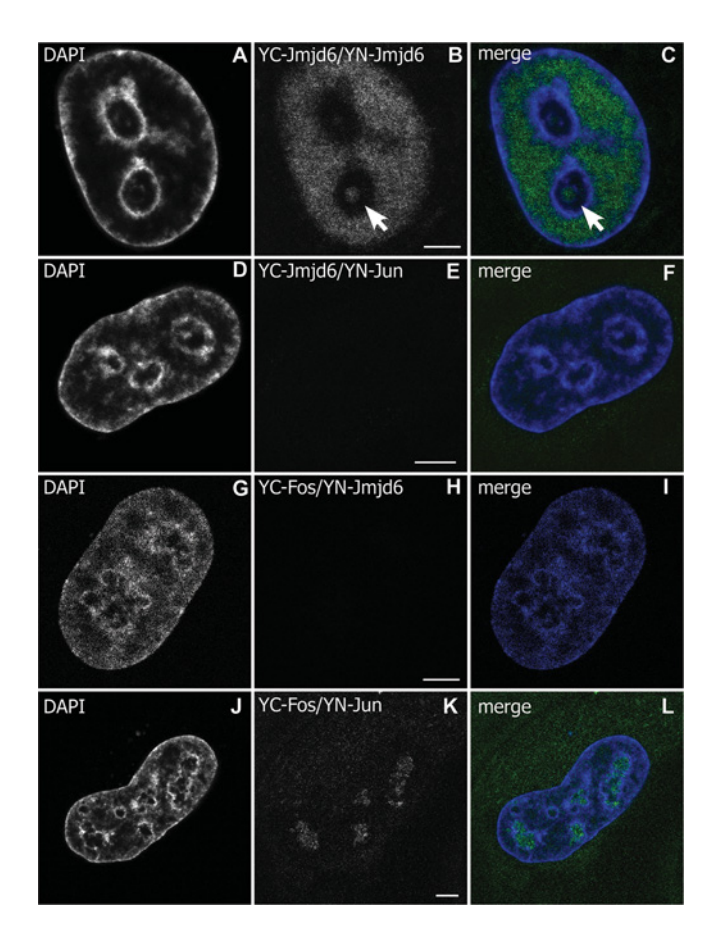


Figure S2 BIFC analysis in HeLa cells demonstrates Jmjd6 dimerization in vivo

Full-length Jmjd6 fused to a N- and C-terminal fragment of YFP (YN-Jmjd6, YC-Jmjd6) respectively were transfected in HeLa cells. (**A–C**) YFP signal displayed Jmjd6 homo-dimerization *in vivo* in the nucleoplasm and also in the nucleoli (indicated by a white arrowhead). For control experiments we used blun and bFos proteins, tagged with YFP fragments. YC-Fos and YN-Jun have been shown to interact in BIFC assays previously [1]. (**J–L**) YC-Fos and YN-Jun gave rise to a YFP-signal in nucleoli, as reported previously [1]. (**D–I**) However, co-expression of YC-Jmjd6 with YN-Jun or YN-Jmjd6 with YC-Fos respectively did not give any YFP signal. DNA was stained with DAPI. Scale bar, 5 μ m.

REFERENCE

 Hu, C. D. and Kerppola, T. K. (2003) Simultaneous visualization of multiple protein interactions in living cells using multicolor fluorescence complementation analysis. Nat. Biotechnol. 21, 539–545

Received 12 April 2013/14 May 2013; accepted 21 May 2013 Published as BJ Immediate Publication 21 May 2013, doi:10.1042/BJ20130529